Renewable and Sustainable Energy Reviews 41 (2015) 189–201

Contents lists available at ScienceDirect

Renewable and Sustainable Energy Reviews

journal homepage: www.elsevier.com/locate/rser

Load monitoring for active control of wind turbines

Aubryn Cooperman *, Marcias Martinez

Faculty of Aerospace Engineering, Delft University of Technology, Building 62, Kluyverweg 1, 2629HS Delft, P.O. Box 5058, 2600 GB Delft, The Netherlands

ARTICLE INFO

Article history:
Received 12 June 2014
Received in revised form
3 August 2014
Accepted 17 August 2014

Keywords:
Load monitoring
Active load control
Fiber Bragg grating
Rayleigh backscattering
MEMS
Lidar

ABSTRACT

This review article examines the range of sensors that have been proposed for monitoring wind turbine blade loads for the purpose of active load control over the past decade. Wind turbine active load control requires sensors that are able to detect loads as they occur, in order to enable a prompt actuation of control devices. Loads may be detected based on structural effects or inferred from aerodynamic measurements. This paper is organized into the following sections: wind turbine control, requirements for load monitoring sensors, sensing technologies and field tests of load control. The types of sensors examined in this article include fiber optic sensors, inertial sensors, pressure measurements and remote optical sensing.

Contents

* Corresponding author. Tel.: +31 15 278 8233.
E-mail address: a.m.cooperman@tudelft.nl (A. Cooperman).

http://dx.doi.org/10.1016/j.rser.2014.08.029
1364-0321/

1. Introduction

Wind turbines are an important source of renewable electricity generation. Worldwide, electricity-generating capacity from wind energy has exceeded 300 GW [1] and it continues to grow, contributing 22% of the new capacity installed in 2011 [2]. As a clean, renewable energy source, wind energy capacity is expected to continue growing.

Wind turbines are not only becoming more numerous but also larger. Increasing the size of individual rotors reduces the total number of turbines needed to produce a given amount of energy. This is particularly important for offshore wind farms where the costs of installing and connecting each foundation are much higher than onshore. Taller turbines also capture more energy from faster wind speeds found higher in the atmosphere. Increased energy capture produces higher aerodynamic loading on the structure, while there is also a need to minimize the structural weight of the blades in order to reduce gravitational loads. Monitoring and controlling these loads will become more important as turbines become larger and are located farther from shore.

Load sources on wind turbines can be described as aerodynamic, operational (caused by control actions), gravitational or inertial (gyroscopic and centrifugal) [3]. The rotor is the source of the most significant loads on the turbine. Reducing loads on the blades also reduces loads throughout the drivetrain and tower [4,5]. Turbines are becoming large enough that rotors span significant changes in wind speed including gusts, low-level jets, wind shear and turbine wakes [6–10]. Many of these affect only a portion of the rotor and require detection and response on a smaller scale than the full blade.

Fig. 1 highlights some of the key locations where sensors may be placed on a wind turbine. The nacelle houses the main electrical components and the controller. Condition monitoring sensors such as vibration sensors and oil contamination monitors may be installed in the nacelle to detect deterioration of the generator and gearbox. An anemometer and wind vane are typically located on top of the nacelle to detect the wind speed and direction. The rotor comprises the blades and rotating hub. Processors, sensor interrogators and LIDAR may be located in the rotating hub. The blade roots are a key location for detecting blade bending moments and also house the pitch drives that orient the blades with respect to the incoming wind. The outboard sections of the blades experience the largest aerodynamic forces, with the largest deflection occurring at the blade tips.

Sensors can be categorized as aerodynamic (inflow) or structural. Inflow sensors provide information about variations in the incoming wind field that produces the loads an active control system seeks to mitigate. They are able to provide measurements before the load occurs, giving the control system and actuators more time to bring the blade into an optimal state [11]. A downside to this approach is the disconnect between the measured quantity and the actual loading experienced by the turbine. Inaccuracy in the model used to correlate inflow measurement and loads can decrease the control system effectiveness and potentially cause instability [12,13]. The accuracy of inflow measurements can be reduced by the evolution of the wind field and variations in the turbine rotational speed between the time of measurement and the time at which the blade interacts with the measured flow. Structural measurements suffer from the opposite problem: loads may be measured accurately but too late to alleviate their effects on the turbine. Structural sensors can detect loads that are not anticipated by a particular model (although optimal sensor positions are facilitated by good modeling of the dynamics).

Structural sensors can also add value by contributing to condition monitoring and structural health monitoring of a turbine. Condition monitoring is expected to be implemented on more turbines in the future, particularly in offshore wind farms where access for maintenance can be difficult. Multipurpose sensors that contribute to structural health or condition monitoring as well as load control systems could provide several benefits. Many of the sensors described in this paper can also be used for condition monitoring [14–16] or structural health monitoring [17–20].

This paper is organized into the following sections: wind turbine control, requirements for load monitoring sensors, sensing technologies and applications to load control.

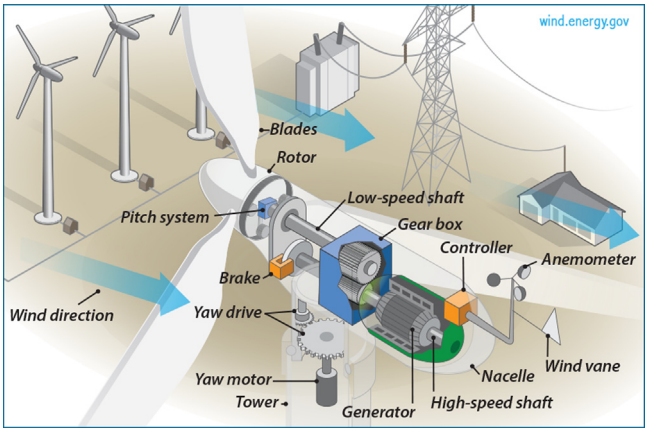

Fig. 1. Wind turbine schematic.
Source: US Department of Energy

2. Wind turbine control

This section gives a brief outline of control systems in modern wind turbines; for more in-depth discussion on the subject see references such as [3,21,22]. Wind turbines require control for several purposes: to ensure safe operation of the turbine, to maximize power production and to minimize extreme and fatigue loading of the structure. Each of these goals is prioritized in different regions of the turbine's operational range as shown in the idealized power curve in Fig. 2. Supervisory control is responsible for start-up and shutdown of the turbine, both under normal conditions in Regions 1 and 4, as well as in abnormal conditions such as a grid fault [22]. Operational control in Region 2 seeks to maximize power output, while in Region 3 the power output is held constant at the rated power in order to limit loads. The change from Region 2 to Region 3 encompasses some of the most significant loads on the turbine, so some controllers define a Region 2.5 in order to smooth the transition. Another transitional region (Region 1.5) is sometimes defined at low wind speeds where the turbine may spin without generating power.

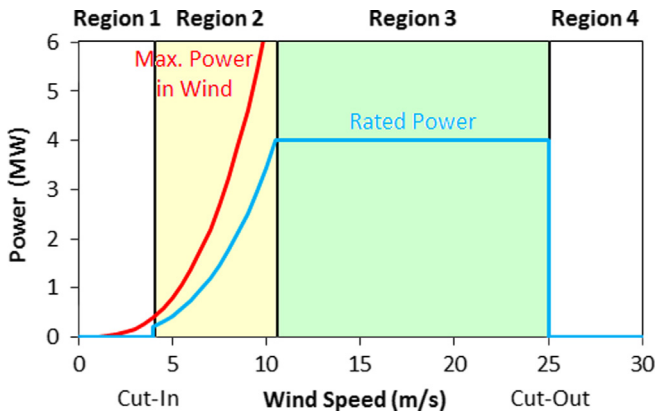

Fig. 2. Wind turbine power curve with control regions. No power is generated below the cut-in wind speed in Region 1. In region 2, the controller maximizes power output up to rated power. Rated power is maintained in region 3 up to the cut-out wind speed. Transitional control between Regions 1 and 2 and Regions 2 and 3 may be defined as Region 1.5 and Region 2.5.

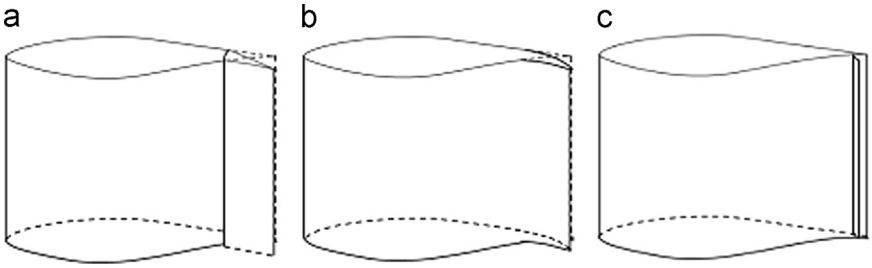

Fig. 3. Active load control concepts: (a) trailing edge flap, (b) flexible trailing edge, and (c) microtab.

Utility-scale wind turbines have evolved from the "Danish model", which was a fixed-speed, fixed-pitch, stall-controlled turbine, to today's commercial models which are predominantly variable-speed, variable-pitch turbines. Fixed-speed turbines rotate at a single rate that is determined by the generator configuration and grid frequency. Variable-speed turbines operate over a range of speeds, allowing the controller to seek the optimum tip speed ratio (the ratio between the speed of the blade tips and the wind speed) for maximum power production in Region 2. The rotational speed is controlled by varying the rotor (or generator) torque.

Stall control is a passive mechanism that utilizes the decrease in airfoil lift coefficient at large angles of attack in order to reduce loads in Region 3. In a turbine with variable pitch, each blade is equipped with a pitch motor that can adjust the pitch angle. The pitch rate for large turbines (5–10 MW) is limited to approximately 6–8°/s. Blades may be pitched to stall (higher angles of attack) or to feather (lower angles of attack). Pitching blades to feather avoids the unsteady behavior seen during stall while still reducing loads at higher wind speeds.

As turbine size continues to increase, differences in the wind profile across the rotor are becoming more important. Cyclic pitch addresses these differences by allowing the blade pitch angle to vary with azimuth angle. Individual pitch control also allows for non-cyclical variations in pitch angle, with each blade pitch angle being set independently [23]. Some limitations of individual pitch control include the power required for frequent blade pitching and the low pitch rate dictated by the blades' high inertial mass.

Active aerodynamic load control seeks to address load variations that occur along the span of a single blade, and within shorter time spans compared to the turbine rotation period. Actuation methods proposed for active load control of wind turbine blades include trailing edge flaps [24,25], flexible trailing edges [26], microtabs [27] microjets [28], plasma actuators [29] and bend twist coupling [30]. Some active load control devices are shown in Fig. 3. These devices are often conceptualized as part of a smart rotor. A smart rotor includes sensors, actuators and a control system to optimize the turbine's response to varying atmospheric conditions. The concept of a smart rotor is based on experience in the rotorcraft field [31]. Developments in the research of smart rotors for wind turbines are well-summarized in [32].

3. Sensor requirements for load control

Wind turbines today have remarkably few sensors. Wind speed and direction are typically measured using an anemometer and wind vane on the nacelle. These measurements are affected by proximity to the rotor and do not reflect the undisturbed inflow conditions. The wind direction is input to the yaw controller and the wind speed measurements are used to determine the timing of start-up and shut-down in low and high wind speeds. The rotor speed is the primary control input during normal operation of the turbine, both for torque control in Region 2 and pitch control in Region 3 [22]. Power output, as the principal reason for erecting a wind turbine, is of course also measured.

The operating environment creates several requirements for sensors on wind turbines. Reliability is a key requirement, especially for sensors installed in the blade, where they are only accessible with difficulty. Sensors installed in the blades are expected to be able to operate throughout the typical 20-year lifetime of the turbine with minimal or no maintenance. The difficulty of accessing the blades provides an argument for locating sensors in the nacelle when possible [33], although some studies have found optimal sensor placements to lie away from the blade root [34–37].

Physical characteristics of the sensor should include small size and light weight to facilitate installation and minimize the impact of the sensor on the turbine. The sensors will need to operate in a wide range of environmental conditions including temperatures between −30 and +65 °C and humidity levels from 0 to 100%. If sensors are located on the exterior of the turbine, they will be exposed to sunlight, precipitation and soiling such as dirt and insects. Icing is a concern in many locations. Exterior sensors must either be capable of functioning while coated with several millimeters of ice or be equipped with a heater.

Lightning strikes are a significant risk for wind turbine systems, so lightning survivability or appropriate lightning protection must be considered [38]. Electrostatic discharge may also occur due to the accumulation of charge as the rotor blades travel through the air. Other electrical considerations include multiplexing capability and the avoidance of cross-talk. Communication between rotating and non-rotating frames also requires consideration. Slip rings allow for transfer of data and power between rotating components for a limited number of channels. Wireless devices can eliminate the need to transfer data via slip ring, but still require power. Greater autonomy and signal processing at the point of detection can reduce the power requirements for data transmission. A smart blade should incorporate sensors, control and actuation in a device in the rotating frame.

For all sensors, minimal drift and hysteresis with a repeatable linear signal and high signal-to-noise ratio are desirable characteristics. Requirements for sensor performance—parameters such as sensitivity, accuracy and range—are predominantly determined by the type of measurement. Sensor response time requirements, however, are driven by the wind turbine system. Important time scales for load control include the aerodynamic response time for the local flow, the dominant blade and tower vibrational modes, and the per-revolution turbulent excitation frequencies (1P, 2P, 3P) [39]. As an illustration, relevant time scales for the NREL 5 MW turbine are given in Table 1. The system natural frequencies given in Table 1 do not include the effects of wind speed and foundation type, which are examined in detail in Bir and Jonkman [40].

3.1. Wireless sensors

Sensor systems need a power source and a means to communicate their output. If the sensors are located in the rotating

Table 1
Relevant frequencies for load control, NREL 5 MW turbine. Full system and per rev frequencies from [41], local section flow adjustment based on [39].

NREL 5 MW		
Full system natural frequencies		
1st tower (fore-aft and side-side)	0.3 Hz	
1st drivetrain torsion	0.6 Hz	
1st blade flap (yaw, pitch, collective)	0.6–0.7 Hz	
1st blade edge (pitch, yaw)	1.1 Hz	
2nd blade flap (yaw, pitch, collective)	1.7–2.0 Hz	
2nd tower (fore-aft and side-side)	2.9 Hz	
Local section flow adjustment ($5c/U_{rel}$)		
	Cut-In	***Rated***
52% span	1.3 Hz	2.4 Hz
72% span	2.3 Hz	4.0 Hz
91% span	3.7 Hz	6.4 Hz
100% span	4.5 Hz	7.7 Hz
Per rev		
1P	0.1 Hz	0.2 Hz
2P	0.2 Hz	0.4 Hz
3P	0.4 Hz	0.6 Hz

portion of the turbine, wired connections must travel through slip rings. The number of slip ring channels is generally low, particularly for data lines, which has led to interest in using wireless communication. Wireless systems can consolidate the output of several sensors and transmit data using a wireless modem, eliminating the need for individual communication lines between each sensor and a central data processor. Transmission can be interrupted if the signal quality is poor, so a wireless sensor system needs to be able to identify dropped packets for retransmission. In one recent test of a wireless sensor system on a 2 MW wind turbine [42] approximately 5–6% of the data packets from the wireless sensors in the upper portion of the tower required multiple attempts to transmit to the base of the tower.

If power is not supplied via a slip ring, wireless sensors can harvest energy or rely on batteries. Both of these options severely restrict the amount of power available for the sensors. Batteries can only be replaced if they are located in an accessible region of the blade or hub, and frequent replacement is not feasible. Vibrational and solar energy can be harvested to power sensors on a wind turbine [43]. The energy available for harvesting may be minimal, limiting the number of measurements that can be collected or transmitted in a given period [44]. Transmission of the wireless signal is relatively power-intensive, so there is scope to reduce power requirements by pre-processing data before transmission. Data processing algorithms must not be too complex—fast Fourier transforms, for example, can require too much capacity for on-board processing [45].

The design of a control system influences the choice to use wireless sensors. If sensors, actuators and data processing can be co-located then wired connections are simpler. Larger distances or relative rotation between control system components make wireless communication more advantageous.

4. Methods: available sensor technologies

4.1. Strain measurements

Strain measurements are a fundamental method for monitoring loads on a structure. Strain measurements on a wind turbine typically focus on the blade roots and tower base in order to determine bending moments at those locations. More details of the loading can be obtained by taking measurements at several points along the tower or blades, which is typically done during structural testing of components or field tests of prototype turbines.

Many controllers that have been proposed for active load mitigation on wind turbines use strain measurements as input to the controller, with actuation methods including individual blade pitch [46,47], trailing edge flaps [48–50], or a combination of the two [51]. Andersen et al. [35] investigated the optimal placement of strain gauge sensors for trailing edge flap control. For a single flap (10% span), the optimal strain gauge location was found to be at a radius 44% of the blade length, inboard from the flap position (between 70 and 94% depending on elastic vs. stiff models). The addition of a second and third flap required additional strain gauges, whose optimal locations were also found to be between the blade root and the flap location.

4.1.1. Metallic strain gauges

For many applications, bonded metallic strain gauges are the most common tool for strain measurement due to their low cost, wide availability and well-understood properties, but they have several disadvantages for load monitoring on wind turbines. The most important problem is the difficulty of obtaining accurate measurements over a long term. The thin foil or wire used in metallic strain gauges ages rapidly, causing the readings to drift and eventually requiring replacement due to fatigue. Results of one field test using metallic strain gauges on a wind turbine reported that gauge excitation voltage offsets had to be reset after six weeks of testing because the drift was large enough to cause signal clipping [52]. Another study estimates the typical lifetime of metallic strain gauges on a wind turbine rotor at 1–3 years [53]. Temperature compensation can be another significant source of error in strain gauge measurements [54]. The measured strain is affected by thermal expansion of both the strain gauge and the component being monitored; compensation is made more difficult by the mismatch in material properties between the composite blades and metallic gauges. Metallic strain gauges are typically used in a Wheatstone bridge configuration, which doubles the number of wires leading to each sensor location. Large wire bundles may be problematic for installation and maintenance and can also be vulnerable to electrostatic discharge on the blade [55]. Finally, metallic gauges are limited to measurements of surface strain, as they are too large to embed in composite materials without disrupting the local strain distribution [17].

Despite the disadvantages of metallic strain gauges for long term load monitoring, they have been applied over shorter periods to several measurement campaigns for testing of active control strategies [e.g. [52,56,57]].

4.1.2. Piezoelectric strain sensors

Piezoelectric materials have the property that mechanical stress generates an electrical field, or conversely that electrical input can prompt a mechanical response. Piezoelectricity is a natural property of some materials such as quartz crystals and can be induced in manufactured materials including piezoceramics such as PZT and polymers such as polyvinylidene fluoride (PVDF) [58]. The use of piezoelectric materials has led to the existence of many types of piezoelectric sensors and actuators such as active fiber composites (AFC) [59], stack actuators [60], and macro fiber composites (MFC) [61,62] to name a few. As sensors, piezoelectric materials have the advantage of not requiring an external power source or intermediate signal processing to produce electrical output [63]. Piezoelectric sensors are used to detect various mechanical quantities including strain, acceleration and pressure. They are best suited to measuring dynamic quantities because the electrical output decays under static conditions.

Piezoelectric strain sensors have been used in wind tunnel tests of active load control systems at TU Delft. Initially, PZT patches were used to measure strain at the root of a blade in a low-speed wind tunnel [25]. The flapwise bending moment was used as the input to a feedback controller for reduction of fatigue loads. Next, a rotating small-scale turbine (rotor diameter = 1.8 m) was built for testing in TU Delft's Open Jet Facility [64]. Two types of piezoelectric strain sensors—PVDF and MFC—were compared with conventional metallic strain gauges as candidates for input to the control system. PVDF sensors were found to be too sensitive to electromagnetic interference, while the MFC sensors had a higher signal-to-noise ratio and were chosen for tests of the scaled smart rotor. The out-of-plane bending strains measured by MFC sensors at each blade root were used to control trailing edge flaps on each blade. Several feedback and feedforward controllers were compared and the best-performing controller was estimated to reduce the flapwise moment fatigue loads by 50.5% [65,66].

4.2. Fiber optic sensors

Optical fiber offers several advantages for sensors in wind turbine blades. They are lightweight and flexible, and can be embedded in composite materials or attached to a surface. Optical fiber sensors do not require an electrical current at the sensing location and are immune to electromagnetic interference [67]. The communications industry has provided a large market for fiber optic products, leading to lower costs for fiber optic sensors.

Several variables can affect the transmission of light through optical fibers. Strain and temperature are the principal measurands of the sensors discussed here, but deflection, pressure, acoustic vibrations and chemical changes can also be measured using fiber optic sensors. Fiber optic sensors may be "point" sensors that give information about a single spatial location, "integrated" sensors that output a single value for an entire fiber (e.g. total strain), "distributed" sensors that measure distributed properties with fine spatial resolution or "quasi-distributed" sensors that provide an assemblage of several point measurements distributed along a fiber [68].

Optical fiber may be either silica (glass) or polymer (plastic). Silica optical fibers are made from the same material as the fiber matrix in most composite blades, although the optical fibers are larger in diameter. Their strain response and sensitivity to environmental factors is therefore similar to that of the blade structure, as is their lifetime. Polymer optical fibers exhibit considerable variation of material properties depending on the type of polymer and manufacturing process [69]. They are generally cheaper than silica fibers, but have higher losses, limiting the maximum sensor length. Polymer fibers may degrade over time when exposed to high temperatures (close to 80 °C) or humidity. This is less of a concern for silica fibers, which typically have a protective coating such as polyimide [69].

The simplest method of installing fiber optic sensors is to attach them directly to the surface of a structure such as a wind turbine blade or tower. This allows for retrofitting of sensors as well as application to new turbines. The fibers are easily accessible if maintenance is required, but they are also vulnerable to environmental degradation or accidental breakage. Typically fiber optic sensors are installed on the interior surface of the blade or tower, so that they do not affect the aerodynamic performance of the turbine and are sheltered from sunlight and extreme weather. When bonding optical fibers to a structure, particular care is required in the choice and application of adhesive to ensure good long-term performance and accurate transfer of strain and temperature [70].

The composite material of a wind turbine blade allows fiber optic sensors to be embedded in the blade, where they are protected by the material and are able to provide information about strain within the structure, not only its surface. Embedded fibers can also be used during the manufacturing process for cure monitoring and quality control [17]. Although embedding optical fibers in composite materials has several advantages, there are also difficulties involved. Care must be taken when embedding fibers to avoid "resin eyes" that weaken the composite structure and microbends that destroy the sensor output, and to make good contact with the composite material to ensure transfer of strain and temperature [55,71,72]. The ingress or egress points of an embedded fiber are vulnerable to breakage during transportation and assembly, and embedded fibers cannot be replaced if broken.

Fiber optic sensors require an interrogator to detect and interpret optical signals. The interrogator can be located in the blade or rotating hub, which provides the best optical signal quality to the detector. In smaller turbines where interrogators cannot easily be located within the blades, a fiber optic rotary joint can be used to connect rotating sensors to a stationary detector [73,74].

4.2.1. Fiber optic strain sensors

Several types of fiber optic strain sensors are discussed briefly here; more detailed information is available in other sources [e.g. [67,75]].

4.2.1.1. Intensity-based sensors. The simplest fiber optic sensors measure the reduction in the intensity of transmitted light that occurs when a fiber is bent. Intensity-based sensors can be used to measure deflection [76] or microbends can be introduced in a fiber for the measurement of strain. Initial steps were taken in the development of a microbend strain sensor for wind turbine blades [77], but further development was discontinued in favor of fiber Bragg gratings after their price dropped steeply [14]. Intensity-based sensors also have the disadvantage that they cannot be multiplexed.

4.2.1.2. Fiber Bragg gratings. A fiber Bragg grating (FBG) is a periodic variation in the index of refraction within an optical fiber. The variation is caused by exposing the fiber to light at a wavelength to which it is photosensitive [78]. A common method for producing fiber Bragg gratings is the phase mask technique, which uses an etched glass "mask" to refract ultraviolet light into the fiber at the prescribed grating size. The wavelength reflected by a Bragg grating is determined by the grating spacing and the refractive index of the fiber. The refractive index varies with temperature and strain, and also—with lower sensitivity—to pressure changes and acoustic signals, altering the reflected wavelength [79]. FBGs can be arranged into rosettes for multi-directional strain measurements.

The relationship between the Bragg wavelength and strain does not need to be recalibrated after installation and it remains stable over time. However, changes in temperature affect the strain readings and temperature compensation is required for accurate measurements. This can be achieved by installing pairs of FBGs in parallel, with one sensor in thermal contact with the structure but isolated from strain. Strain data from the other sensor can then be compensated based on the measured temperature. Combining measurements from silica and polymer FBGs can improve the ability to distinguish between temperature and strain effects, especially if a polymer with a negative temperature sensitivity is used so that a change in temperature causes opposite responses in the silica and polymer fibers [80].

Multiplexing of FBGs can be accomplished by time division multiplexing (TDM), wavelength division multiplexing (WDM), or a combination of the two methods [67]. Both techniques enable several FBGs to share a single fiber. In time division multiplexing light enters the fiber as discrete pulses, which are reflected back to

the detector at different times based on the distance of each grating from the source. In wavelength division multiplexing, the spacing of each grating is chosen to reflect a different wavelength. The sampling rate for WDM can go up to a few kHz, while for TDM it depends on the number of sensors and the pulse travel time. The number of sensor points is limited by the source bandwidth and the frequency resolution of the detector when using WDM and by signal attenuation for TDM, with WDM typically allowing for fewer measurement points than TDM [81].

Embedded FBG strain measurements in composite structures have been validated by comparison with conventional strain gauges and finite element modeling [82,83]. Initial field tests of FBGs for load monitoring retrofitted surface-mounted sensors onto existing turbine blades. Strain measurements at the blade root were found to correspond well with measurements taken by co-located conventional strain gauges [84,85].

Several field tests have taken advantage of FBGs' multiplexing capability to obtain semi-distributed strain measurements [85–88]. A typical arrangement includes five or six sensors per fiber for either wavelength or time division multiplexing. Modal analysis of a blade based on semi-distributed strain measurements can be used to determine the deformation shape [89,90] or for damage detection [91].

4.2.1.3. Rayleigh backscattering. Backscattering refers to light that is reflected (scattered) back to its origin due to randomly-distributed variations in the refractive index of an optical fiber, caused by inhomogeneities in the fiber. Several types of backscattering occur in optical fiber; depending on the wavelength of the backscattering it can be subdivided into three specific types of peaks known as the Rayleigh, Raman and Brillouin peaks. Rayleigh backscattering creates more energetic peaks than Raman or Brillouin backscattering and is therefore easier to detect [92]. The spectrum of the backscattered pattern varies as the shape and density of the fiber change due to bending, twisting, strain and temperature changes.

Rayleigh backscattering can measure strain and temperature in both silica and polymer optical fibers [94,95]. There are two main approaches to sensors using backscattering: optical time-domain reflectometry (OTDR) and optical frequency-domain reflectometry (OFDR). OTDR measures variations in amplitude of the reflected signal over time, while OFDR measures phase shifts. OFDR has higher resolution of strain and temperature but is limited to shorter fiber lengths due to measurement noise. OTDR can be used for fibers up to several kilometers in length, while OFDR is feasible for fiber lengths up to 100 m [92]. The acquisition period for OFDR sensors is too long for dynamic measurements, but it has been applied to static tests of wind turbine blades. [92,96]. The OFDR technique can be used with multi-core optical fibers to determine deformation of a structure in three dimensions [97].

4.3. Inertial sensors

Inertial sensors detect the motion of a structure that results from forces applied to the structure. The most commonly used inertial sensors are accelerometers, but velocity, rotation and displacement may also be measured. Accelerometers measure linear acceleration along a single axis, or they may comprise three orthogonal devices in a single package, creating a tri-axial accelerometer. Acceleration data can be integrated twice to determine the displacement of the structure. The introduction of two integration constants makes signal drift a significant concern for estimation of the total deformation.

The basic architecture of an accelerometer includes a proof mass, which is attached to a spring and damper and whose motion is detected by a sensing element. The sensing element may be either passive or active. Passive accelerometers incorporate a piezoelectric material that deforms as the proof mass moves, emitting an electrical signal. In active accelerometers, the motion of the proof mass alters an electrical property of the system—commonly by changing the distance between the plates of a capacitor. The change in capacitance can only be detected if the electrical circuit is powered. Piezoelectric systems respond to changes in acceleration, but if the level of acceleration remains constant (e.g. gravitational acceleration in a static system or centripetal acceleration at a constant rotational speed) they discharge over time. Active accelerometers measure both constant and dynamic acceleration, but with a lower signal-to-noise ratio than passive accelerometers.

Operation on a rotating system poses a challenge for acceleration measurements because the centripetal acceleration may be much larger than the acceleration due to dynamic loading. White et al. [98] described a method for estimating sensor rotation using the ratio of the spanwise and out-of-plane acceleration terms. Several sensor measurements are combined for an estimation of the tip deflection. The measurement scheme was implemented on an instrumented 9 m rotor blade, however, the accelerometers failed in field tests due to electromagnetic discharge [99]. Accelerometers have been proposed as a sensor for trailing edge flap control [100]. Blade-mounted accelerometers have also been used to detect damage during fatigue tests [101] and to detect rotor imbalance [102]. Accelerometers must be placed to capture the principal blade vibrational modes to obtain the best sensitivity. Several studies have investigated optimal sensor placement of inertial sensors [34,36,103].

4.3.1. Microelectromechanical systems (MEMS)

Microelectromechanical systems (MEMS) combine mechanical and electrical components on a scale of microns to millimeters. Integrated circuit fabrication techniques are used to produce a wide variety of MEMS devices [104,105]. Common MEMS sensors include strain gauges, accelerometers, pressure sensors and gyroscopes. In comparison with more traditional versions of these sensors, MEMS are smaller and lighter, with lower power requirements and often a lower cost. These attributes simplify the installation of a network of sensors within a structure; however, MEMS sensors tend to have lower precision and range than larger devices. While the highest precision aerospace accelerometers are bulk devices, MEMS accelerometers have become common in the automotive industry and in mobile devices (among other applications). Gyroscopes and accelerometers can be combined as inertial measurement units, and some MEMS also incorporate magnetometers for global orientation. Martinez et al. [106] investigated the use of MEMS combining gyroscopes, accelerometers and magnetometers as a potential technique for determining the shape of a structure, which in combination with finite element methods allows for the computation of strain and stresses over the structure.

4.4. Local aerodynamic sensors

4.4.1. Pitot tube

A pitot (or pitot-static) tube is a standard instrument for measuring air speed on commercial aircraft, so they are well-studied and available from several manufacturers. In its simplest form, a pitot tube has two holes for pressure measurement: one at the end of the tube perpendicular to the oncoming flow, and one on the tube's side. At the base of the tube, a differential transducer compares the pressures (total and static, respectively) obtained at the two holes and Bernoulli's principle is used to determine the

velocity. More complex probes may have several holes at the tip—usually 5 or 7—to allow determination of the local angles of attack and sideslip.

Pitot tubes must be mounted forward of an airfoil section, pointing into the airflow. This mounting arrangement can have several disadvantages. The boom holding the tube is kept narrow to minimize its impact on the airflow, but this leaves it subject to vibration and bending, which causes measurement error. The local inflow angle measured by a pitot tube differs from the blade section angle of attack due to upwash induced by the bound vortices on the blade. Correction methods have been developed for horizontal axis wind turbines [107,108]. Pitot tubes are exposed to precipitation, ice, dirt and insects, all of which can enter the pressure tubing and disrupt measurements and may require manual cleaning to remove.

Controllers have been developed for cyclic and individual pitch control based on local angle of attack and relative velocity measurements using pitot tubes [11,109,110]. Trailing edge flap controllers have also been based on inflow measurements using 5-hole pitot probes [111,112]. Fischer and Madsen [37] used field measurements to evaluate the maximum load reduction potential of trailing edge flaps based on measurements from four 5-hole pitot tubes. An inverse relationship was found between the sensor-to-flap distance and the achievable controller bandwidth. This relationship did not depend on the blade length, suggesting that larger blades will require more pitot tubes to cover the full blade.

Pitot tube length can be a factor in the accuracy of the sensor, with longer tubes subject to more bending and vibration, while shorter tubes are more strongly influenced by upwash. Heinz et al. [113] compare control based on the local angle of attack measured by pitot tubes of varying lengths in 2D simulations of a wind turbine airfoil with an adaptive trailing edge flap. The maximum load reduction is obtained for the shortest pitot tube length, 5% chord. The longer pitot tubes experience a larger range of motion during turbulent inflow, which reduces the measurement accuracy. In 2D wind tunnel tests of a deformable trailing edge flap, the shortest pitot tube tested (50% chord) was also found to perform better than longer pitot tubes due to the motion of the airfoil [114].

4.4.2. Surface pressure

Surface pressure measurements may be made using surface-mounted transducers or by connecting several surface taps to a scanning pressure transducer. Surface-mounted transducers minimize the error associated with transferring pressure over a distance and can accurately measure dynamic pressure data; however, it is expensive to provide a pressure transducer for a large number of measurement sites and the miniature transducers used for surface measurements can be fragile and easily damaged. Scanning pressure transducers can reduce costs and maintenance requirements by measuring several (commonly 32, 64 or 128) pressures with a single transducer. The frequency response of the sensor is affected by the distance between the surface pressure tap and the transducer. Large distances cause delay and distortion of the pressure signal, reducing the accuracy of high frequency measurements. Filtering techniques can be used to reconstruct the original pressure signal [115].

Increasing the number of surface pressure taps can improve the accuracy of aerodynamic force estimation on a blade section, but also adds to the expense and complexity of installation and data processing. The NASA flush air data sensing (FADS) system detects pressures at three points on the airfoil surface, on the leading edge, upper and lower surfaces [34]. The system can measure the angle of attack and sideslip, as well as the freestream and dynamic pressures. Olsen et al. [116] also discussed a similar system for pressure and angle of attack measurement. An individual pitch control system based on angle of attack measurements produced significant reductions in the blade root bending moments (-38% flapwise max) compared with a PID controller [116].

Gaunaa and Andersen [12] proposed the pressure difference between the upper and lower surfaces of a simulated 2D airfoil at one or two chordwise locations as a control input for trailing edge flaps. Using thin airfoil theory, the preferred location for surface pressure measurements was found to be at 12.5% chord. Control systems for trailing edge devices based on a surface pressure difference have been tested in 2D simulations [113] and in wind tunnel experiments [114,117,118].

4.5. Remote inflow sensors

Light detection and ranging (LIDAR) and similar technologies offer the ability to "preview" the incoming wind field, which could allow for more optimal control of the system. LIDAR (more specifically, coherent Doppler LIDAR) uses coherent light produced by a laser, which is reflected back to the LIDAR by particles suspended in the atmosphere such as dust, pollen, or water droplets. The reflected light is analyzed in an interferometer to detect Doppler shifts and determine the speed of the particles with respect to the beam axis. LIDAR was first developed in the 1970s, but early systems required cryogenically-cooled carbon dioxide and stable optical alignment. Advances in fiber-based optical systems have made LIDAR more robust and portable and reduced the cost, making turbine-mounted LIDAR feasible [119]. Several studies have investigated the potential of LIDAR preview measurements for wind turbine control [110,120–130].

LIDAR is generally immune to interference from other light sources such as sunlight, but precipitation introduces measurement error because it has a vertical velocity component that does not follow the wind. Moving objects (birds, insects, etc.) can cause false readings, but these are typically infrequent and easily identifiable. On the other end of the spectrum, exceptionally clear days may also be a problem because there are not enough particles in the air from which to scatter.

LIDAR systems may be either continuous wave (cw) or pulsed. Pulsed systems provide wind speeds at multiple distances from the turbine nearly simultaneously, based on backscattering of the pulse. Continuous wave LIDARs focus the laser beam at single distance. Typical ranges are a few hundred meters for cw LIDAR or up to tens of kilometers for pulsed LIDAR [119]. The output rate of a pulsed system is on the order of 1 Hz, while cw systems can have an output rate of around 50 Hz [131]. Varying the focal length can alter the frequency response of a cw LIDAR. Increasing the focal length decreases the frequency response by averaging the velocity across a larger measurement area, which has an effect similar to decreasing the cut-off for a low-pass filter.

When used for site assessment or wind profile measurements, LIDARs are often positioned on the ground looking upwards. For load control purposes, a LIDAR system may be installed on top of the nacelle or inside the rotating hub. In order to capture data across an area, the LIDAR can be swept through a pattern—often a cone. Mounting a LIDAR system on the nacelle simplifies installation, power and data transmission, but the laser line-of-sight is blocked by the rotating blades approximately once per second. Rotating hub-mounted systems are more complex to install and they require wireless communication or slip rings to transmit data and power, but they have an unrestricted view and can use the turbine's rotation to scan a conical pattern with no additional effort.

Any LIDAR system suffers from the "cyclops effect", a measurement ambiguity caused by the fact that the LIDAR detects only a single wind speed component aligned with its line-of-sight. If the LIDAR is not pointed directly into the oncoming wind,

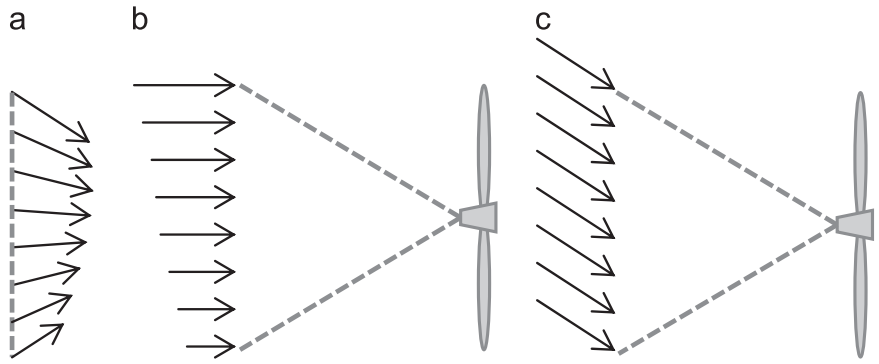

Fig. 4. Illustration of the cyclops effect. Measured wind components across a horizontal scan line (a) are interpreted using the assumption of (b) purely axial wind or (c) homogeneous horizontal wind.

measurement of the axial wind speed will include vertical and sideways components. One of two sets of assumptions is commonly used to deal with the cyclops effect: either purely axial wind or homogeneous horizontal wind [132]. In both these cases, there is assumed to be no vertical component to the velocity, although there may be vertical shear. Variations across the horizontal plane of the measured wind field are assumed to represent horizontal shear for purely axial wind, or yaw misalignment for homogeneous horizontal wind (see Fig. 4). These assumptions are less applicable in complex terrain, where they lead to errors of around 10% in measured wind speeds [132].

Using LIDAR to preview the incoming wind field is only useful if the turbulent eddies seen approaching the turbine are the same or closely related to the eddies that will cause the loads to be controlled. This is the motivation for Taylor's frozen turbulence hypothesis, which suggests that turbulent structures are simply convected along in an unchanging or “frozen” state at the average velocity of the wind field. Although turbulent structures are known to evolve over time, Taylor's hypothesis is commonly used in simulations to simplify computations. While it is possible to avoid the assumption of frozen turbulence in simulations [133], field tests [134] suggest that the hypothesis is valid for eddy length scales on the order of 0.1–2 rotor diameters for multi-megawatt turbines.

The optimal preview time (or, equivalently, the focal distance) for a nacelle-mounted LIDAR depends on the details of the control system, but also varies with the wind speed. As the wind speed increases, longer preview times and larger focal distances become more advantageous, until a maximum preview time is reached beyond which the control system performance does not improve [135,136]. Turbulence and evolution of turbulent structures shorten the optimal preview time; however, very short preview distances can only be achieved if the direction of a nacelle-mounted LIDAR makes a large angle with the oncoming wind, nearly in line with the blades and creating a significant directional bias [131].

4.5.1. Other remote inflow sensors

Particle image velocimetry, Doppler global velocimetry and laser Doppler anemometry are techniques used in wind tunnel experiments to measure flow speed and direction. Each of these techniques requires the flow to be seeded with particles to reflect a larger percentage of the emitted laser light than would be obtained in normal atmospheric conditions [119].

Sonic detection and ranging (SODAR) is similar to LIDAR except that pulses of sound rather than light are sent out and reflect back to the detector. A SODAR transmits pulses of sound in the 2000–4000 Hz range and uses a directional microphone to detect scattered return [132]. Pulses are sent in three (different but not necessarily orthogonal) directions for a 3D wind vector. Alternatively, the transmitted signal may be detected at a separate receiver, which significantly improves the carrier-to-noise ratio but only provides 1D information [132]. Sampling rates for SODAR are limited to 0.1–0.17 Hz, and results are typically averaged in 10-minute intervals to determine the mean wind speed and direction. Wind speeds above 15 m/s can cause high background noise, degrading the signal-to-noise ratio. Measurements are also affected by reflections from solid objects.

A summary of sensor technologies discussed in this review article can be found in Table 2. The table highlights advantages and disadvantages of many of these sensors, with their corresponding measurand, sensing frequency, range and resolution.

4.6. Load monitoring sensors in aerospace applications

Detection and response to changing load conditions are also of interest to the aerospace industry. Some of the challenges encountered are similar to those seen on wind turbines and may share similar solutions. Operational flight load monitoring is performed by measuring flight state parameters (pitch, roll, yaw, accelerations, altitude, control surface deflection air speed, etc.) in combination with strain in critical locations of the structure. In flight test aircraft, many strain gauges are utilized to generate the response equations. Load monitoring systems based on strain gauge sensors, however, present certain problems: the gauges themselves become damaged by fatigue and they require complex wiring networks to be installed and maintained to enable the use of all necessary sensors. In the case of unmanned aerial vehicles (UAVs), the weight of the wires becomes so heavy that their installation and usage is prohibitive [137]. Although strain gauges have been considered the gold standard for industrial and commercial applications, their wide use has also highlighted their susceptibility to fatigue and electromagnetic interference. The aerospace community is therefore looking at the use of other sensors based on deflection and shape sensing.

A review of fiber optic systems [138] found that the majority of the research was directed to measuring strain and temperature. These two parameters are crucial in evaluating the structural performance of aerospace and wind energy structures in operational conditions. NASA Dryden used over 3000 fiber Bragg Grating sensors for load monitoring on the Predator-B unmanned aerial vehicle in 2008. The FBGs were used to measure the strain on the wing of the aircraft during flight. In addition, the shape changes of the UAV wing were also measured during the same flight test program. In more recent years, the academic community has been investigating the application of morphing structures in order to improve structural and control performance of UAVs [139]. Fiber optic shape sensors have been applied to morphing structures to monitor the change in shape [140].

Table 2
Comparison of sensor technologies. Range, resolution and frequency values are representative of manufacturers' specifications rather than theoretical limits on the technologies.

Sensor Type	Typical locations	Advantages	Disadvantages	Measurand	Range	Resolution (% FS)	Max. freq. (Hz)
Strain sensors							
Metal-foil gauges	Blade (root), tower (base)	Cheap, widely available, well-understood	Drift, fatigue, thermal sensitivity	Strain	10 to 10,000 με	> 10 με	varies
Piezos		No external power required	Dynamic measurement only	Strain	300 με	0.0002%	0.02
Fiber Bragg gratings (FBGs)	Blade (embedded or surface), tower	Compatible with composite blades, stable over time, multiplexing capability	Thermal sensitivity, fiber handling	Strain	9000 με	0.01%	250
				Temperature	−200 to 300 °C	0.01%	
Rayleigh scattering fiber optics		Compatible with composite blades, stable over time, high resolution distributed measurements	Static measurement only, fiber handling	Strain	15,000 με	0.01%	5
				Deformation	1 to 30 m	1.0%	0.2
Inertial sensors							
Bulk devices	Blade (tip), tower (top)	High accuracy	Gravitational and centripetal acceleration	Acceleration	± 500 *g*	0.0001%	10^4
MEMS		Small, light, low-cost	Gravitational and centripetal acceleration, low resolution	Acceleration	200 *g*	0.01%	100
				Angular rate	2000°/s	0.002%	
				Magnetic field	250 μT	0.1%	
Inflow sensors							
Pressure transducers	Blade	Local measure-ment of wind speed and angle	Soiling, flow interference (Pitot tube)	Pressure	Varies	0.02%	10^5
Pulsed LIDAR	Hub, nacelle	Preview of incoming wind field	Affected by flow evolution, cyclops effect	Wind speed, direction	20 km	0.1 m/s, 0.5°	1
Continuous wave LIDAR					500 m		50

The aerospace community has also considered load-monitoring technologies with a variety of non-contact sensors. For example, the use of Digital Image Correlation (DIC) for load monitoring has been considered in [141]. The results of this work showed how with the utilization of DIC technology, bending and torsional loads could be used to measure the applied loads and moments of a simple structure. Optical techniques including DIC and videogrammetry have been applied to wind turbine monitoring using ground-based cameras [142–144]. For continuous monitoring under conditions of wind direction, a turbine-mounted system would be advantageous. In-flight monitoring also requires cameras to be mounted on a moving system. NASA demonstrated the use of videogrammetry to measure wing deflections of an F/A-18 during flight [145].

5. Experience in field tests

5.1. Inflow measurements

The DAN-AERO project [146] conducted field measurements on a 3.6 MW wind turbine. One blade was instrumented with surface pressure taps at four radial stations as well as four pitot tubes and an array of microphones at the surface near the tip. The inlets to all of these sensors were covered with tape every evening of the measurement campaign to protect against rain and moisture.

Medina et al. [147] installed surface pressure taps at nine spanwise locations on one blade of a 2.3 MW turbine. Approximately 60 pressure taps were monitored at each radial position using pressure scanners mounted inside the blade. Four 5-hole probes were also installed on the blade leading edge. Data from the surface pressure and pitot probes were wirelessly transmitted to a central computer. In order to obtain good quality pressure measurements, the pressure sensors were housed in temperature control units and placed no farther than 25 m from the center of the hub, thereby limiting the rotational acceleration of the sensors. The sensor placement imposed a requirement for long lengths of tubing to the outer pressure taps, which in turn created a need for a filter to compensate for distortion of the pressure signal. Compensation of the pressure signal is discussed in detail in Medina et al. [148].

While ground-based LIDAR is widely used for wind resource measurement, fewer LIDARs have been mounted atop turbines. Field tests of a spinner-mounted LIDAR were conducted at Risø by Angelou et al. [149] (also see [150] and [151]). The LIDAR was installed in the rotating hub of an 80 m diameter rotor, aligned with the turbine shaft axis. Circular scan patterns with two different cone angles were used. The measurements were used to determine yaw error and power curves.

5.2. Wind turbine load control

While many load control and sensing systems are still in development, field tests on a few systems have provided valuable information on the use of sensors for load control applications.

The Controls Advanced Research Turbines (CART2 and CART3) at the National Wind Technology Center in Colorado have been used for testing of advanced load control methods including predictive control and individual pitch control [47,152–154]. As research turbines, they are equipped with a wide range of sensors, including blade and tower strain gauges, accelerometers and pressure transducers, anemometers and wind vanes [155]. Maintaining all of these sensors while operating experimental control systems has required the development of fault detection strategies that may be applicable to future smart rotor systems [156].

Nacelle-mounted LIDAR has been used in field tests for wind turbine speed regulation [157]. A pulsed LIDAR was mounted on a rear guard-rail atop the nacelle of the CART3 research turbine. A feed-forward controller for blade pitch was implemented using LIDAR measurements of the incoming wind field. The feed-forward controller operated in conjunction with the standard feedback controller based on the generator speed, and produced a reduction in the tower fore-aft bending, blade root flapwise bending, and rotor torque compared with feedback-only control. Slight increases were seen in the tower side-side bending and blade edgewise bending moments with the feed-forward controller.

Castaignet et al. [158] replaced one blade of a Vestas V27 turbine with an instrumented blade that had three trailing edge flaps. Sensors on the blade included three 5-hole pitot tubes, pairs of pressure taps located ahead of each flap, and two 3D accelerometers at the tip of the blade. All three blades had two strain gauges (flapwise and edgewise) at the blade root. Initially the effects of prescribed flap deflections were studied. A control system was later implemented using the mean wind speed and the blade root flap moment as inputs [56] for control of a single trailing edge flap. The control system sought to minimize the blade root flapwise fatigue loads at frequencies of 1P and higher, using model predictive control [159].

A smart rotor including sensors, actuators and control was installed at a test turbine in Bushland, TX in 2010 [160]. The blade was instrumented with accelerometers, fiber-optic strain, metal foil strain and fiber-optic temperature sensors, pressure taps and pitot tubes. Triaxial and uniaxial accelerometers were mounted at 2 and 8 m along the 9 m blade. Strain gauges were installed at the root and 25, 50 and 75% spanwise stations. Previous tests had shown that the accelerometers were very susceptible to damage from electrostatic discharge due to lightning or the triboelectric effect [55], so lightning protection (copper wire from tip to hub) and a wire mesh covering the entire blade surface below the gelcoat were added to the blade during manufacturing. In addition, the accelerometers were chosen to have a higher resistance to electrostatic discharge and mounted on grounding blocks.

Aerodynamic sensors on the smart rotor included a five-hole pitot tube and a surface pressure array [160]. A bend was incorporated into the pitot tube to align it with the nominal angle of attack at that blade location (7.9 m or approx. 90% span), to maximize accuracy and range. Reference pressure sensors were located in each blade rather than in the hub to eliminate the need for a pneumatic slip ring. Data from the aerodynamic sensors was transmitted wirelessly to a control building. However, the aerodynamic sensors were not used due to difficulties with the pressure scanner [52]. Tests conducted with the smart rotor included static deployment of the trailing edge flaps and periodic flap motion [39]. Changes in the flapwise strain were observed to correspond to flap deployments [161]. Data from open-loop flap activation were used to simulate the effects of controlled flap activation for load reduction [162].

6. Conclusions

Many different types of sensors have potential for load monitoring on wind turbines. These include structural sensors such as strain sensors, accelerometers and shape sensors, and inflow sensors such as pitot tubes, pressure transducers and LIDAR. Structural sensors can be highly accurate but only respond to loads after they occur. Inflow sensors detect changes sooner, but are sensitive to errors in the models that relate aerodynamic variables to loads. The evolution of turbulent wind fields also poses challenges for predictive sensors like LIDAR, where a balance must be struck between early warning and accurate prediction.

The wind turbine environment produces challenging operating conditions for load sensors. Access and maintenance are difficult and the sensors may be exposed to precipitation, ice, dirt, insects and lightning. The development of robust sensor technologies for wind turbines is needed in order for load monitoring to be widely implemented. Load monitoring sensors do not need to be developed in isolation. Condition monitoring and structural health monitoring of turbines are receiving more attention as means of maximizing wind farms' lifetime and productivity. Sensors for these tasks face many of the same requirements as sensors for control systems, and in some cases the same sensors may be used for both tasks.

Sensors will become increasingly important as larger wind turbines adopt new strategies such as active load control. In order for new sensor technologies to gain acceptance in the wind industry, simple and reliable systems are needed that can provide an accurate assessment of the loads experienced by a turbine. If these goals can be accomplished, improved monitoring of wind turbines will provide opportunities for advanced control and improved performance.

Acknowledgments

Dr. Martinez and Dr. Cooperman would like to acknowledge the funding received through the FP7 Marie Curie Career Integration Grant titled: Monitoring of Aerospace Structural Shapes (MASS) (Grant no. 618316) and the Far and Large Offshore Windpower (FLOW) Project funded by the Dutch Ministry of Economic Affairs. The authors would also like to thank Gijs van Kuik for his valuable comments while preparing this review.

References

[1] Global Wind Energy Council. Global Wind Statistics 2013; 2014.
[2] US Energy Information Administration. International Energy Statistics; 2014.
[3] Burton T, Sharpe D, Jenkins N, Bossanyi E. Wind energy handbook. New York: Wiley; 2001.
[4] Berg DE, Wilson DG, Resor BR, Barone MF, Berg JC, Kota S, et al. Active aerodynamic blade load control impacts on utility-scale wind turbines. Chicago, IL: AWEA WINDPOWER; 2009.
[5] Berg D, Resor B, Wright Z, Halse C, Crowther A. Wind turbine structural path stress & fatigue reductions resulting from active aerodynamics. Anaheim, CA: AWEA WINDPOWER; 2011.
[6] Fragoulis A. The complex terrain wind environment and its effects on the power output and loading of wind turbines. In: AIAA aerospace sciences meeting. Reno, NV; 1997. http://dx.doi.org/10.2514/6.1997-934.
[7] Kelley ND, Osgood RM, Bialasiewicz JT, Jakubowski A. Using wavelet analysis to assess turbulence/rotor interactions. Wind Energy 2000;3:121–34. http://dx.doi.org/10.1002/we.33.
[8] Hand MM, Kelley ND, Balas MJ. Identification of wind turbine response to turbulent inflow structures. In: Proceedings of the 4th ASME/JSME joint fluids engineering conference. Honolulu, HI; 2003. http://dx.doi.org/10.1115/FEDSM2003-45360.
[9] Eggers AJ, Digumarthi R, Chaney K. Wind shear and turbulence effects on rotor fatigue and loads control. J Sol Energy Eng 2003;125:402–9. http://dx.doi.org/10.1115/1.1629752.
[10] Sathe A, Mann J, Barlas T, W.A.A.M. Bierbooms, van Bussel GJW. Influence of atmospheric stability on wind turbine loads. Wind Energy 2013;16:1013–32. http://dx.doi.org/10.1002/we.1528.
[11] Larsen TJ, Madsen HA, Thomsen K. Active load reduction using individual pitch, based on local blade flow measurements. Wind Energy 2005;8:67–80. http://dx.doi.org/10.1002/we.141.
[12] Gaunaa M, Andersen PB. Load reduction using pressure difference on airfoil for control of trailing edge flaps. In: Proceedings of the European wind energy conference. Marseille, France; 2009.
[13] Laks J, Pao LY, Wright A, Kelley N, Jonkman B. Blade pitch control with preview wind measurements. In: 48th AIAA aerospace sciences meeting. Orlando, FL; 2010. http://dx.doi.org/10.2514/6.2010-251.
[14] McGugan M, Larsen GC, Sørensen BF, Borum KK, Engelhardt J. Fundamentals for remote condition monitoring of offshore wind turbines. Roskilde (DK): Technical University of Denmark; 2008.

[15] Hyers RW, McGowan JG, Sullivan KL, Manwell JF, Syrett BC. Condition monitoring and prognosis of utility scale wind turbines. Energy Mater 2006;1:187–203. http://dx.doi.org/10.1179/174892406X163397.

[16] Hameed Z, Hong YS, Cho YM, Ahn SH, Song CK. Condition monitoring and fault detection of wind turbines and related algorithms: a review. Renew Sustain Energy Rev 2009;13:1–39. http://dx.doi.org/10.1016/j.rser.2007.05.008.

[17] Schubel PJ, Crossley RJ, Boateng EKG, Hutchinson JR. Review of structural health and cure monitoring techniques for large wind turbine blades. Renew Energy 2013;51:113–23. http://dx.doi.org/10.1016/j.renene.2012.08.072.

[18] Ciang CC, Lee J-R, Bang H-J. Structural health monitoring for a wind turbine system: a review of damage detection methods. Meas Sci Technol 2008;19:1–20. http://dx.doi.org/10.1088/0957-0233/19/12/122001.

[19] Fritzen C-P, Kraemer P, Klinkov M An integrated SHM approach for offshore wind energy plants. In: Proceedings of the IMAC-XXVIII. Jacksonville, FL: Society for Experimental Mechanics, vol. 3; 2010. p. 727–40. http://dx.doi.org/10.1007/978-1-4419-9834-7_63.

[20] Rohrmann RG, Thöns S, Rücker W. Integrated monitoring of offshore wind turbines–requirements, concepts and experiences. Struct Infrastruct Eng 2010;6:575–91. http://dx.doi.org/10.1080/15732470903068706.

[21] Bianchi FD, De Battista H, Mantz RJ. Wind turbine control systems: principles, modelling and gain scheduling design. London: Springer; 2007.

[22] Pao LY, Johnson KE. Control of wind turbines. IEEE Control Syst 2011;31:44–62. http://dx.doi.org/10.1109/MCS.2010.939962.

[23] Bossanyi EA. Wind turbine control for load reduction. Wind Energy 2003;6:229–44. http://dx.doi.org/10.1002/we.95.

[24] Basualdo S. Load alleviation on wind turbine blades using variable airfoil geometry. Wind Energy 2005;29:169–82. http://dx.doi.org/10.1260/0309524054797122.

[25] van Wingerden JW, Hulskamp AW, Barlas T, Marrant B, van Kuik GAM, Molenaar D-P, et al. On the proof of concept of a "Smart" wind turbine rotor blade for load alleviation. Wind Energy 2008;11:265–80. http://dx.doi.org/10.1002/we.264.

[26] Bak C, Gaunaa M, Andersen P, Buhl T, Hansen P, Clemmensen K, et al. Wind tunnel test on wind turbine airfoil with adaptive trailing edge geometry. In: 45th AIAA aerospace sciences meeting. Reno, NV; 2007. http://dx.doi.org/10.2514/6.2007-1016.

[27] Yen Nakafuji DT, van Dam CP, Smith RL, Collins SD. Active load control for airfoils using microtabs. J Sol Energy Eng 2001;123:282–9. http://dx.doi.org/10.1115/1.1410110.

[28] Boeije CS, de Vries H., Cleine I, van Emden E, Zwart GGM, Stobbe H,et al. Fluidic load control for wind turbine blades. In: 47th AIAA aerospace sciences meeting. Orlando, FL; 2009. http://dx.doi.org/10.2514/5.2009-684.

[29] Nelson R, Corke T, Othman H, Patel M, Vasudevan S, Ng T. A smart wind turbine blade using distributed plasma actuators for improved performance. In: 46th AIAA aerospace sciences meeting. Reno, NV; 2008. http://dx.doi.org/10.2514/6.2008-1312.

[30] Capellaro M. Aeroelastic design and modeling of bend twist coupled wind turbine blades [dissertation]. Stuttgart: University of Stuttgart; 2013.

[31] Chopra I. Review of state of art of smart structures and integrated systems. AIAA J 2002;40:2145–87. http://dx.doi.org/10.2514/2.1561.

[32] Barlas TK, van Kuik GAM. Review of state of the art in smart rotor control research for wind turbines. Prog Aerosp Sci 2010;46:1–27. http://dx.doi.org/10.1016/j.paerosci.2009.08.002.

[33] Ehlers J, Diop A, Bindner H. Sensor selection and state estimation for wind turbine controls. In: 45th AIAA aerospace sciences meeting. Reno, NV; 2007. http://dx.doi.org/10.2514/6.2007-1019.

[34] Abdallah I. Advanced load alleviation for wind turbines using adaptive trailing edge geometry: sensoring techniques [thesis]. Lyngby, Denmark: Technical University of Denmark; 2006 (Kgs).

[35] Andersen PB, Henriksen L, Gaunaa M, Bak C, Buhl T. Deformable trailing edge flaps for modern megawatt wind turbine controllers using strain gauge sensors. Wind Energy 2010;13:193–206. http://dx.doi.org/10.1002/we.371.

[36] Berg J, Miller K. Estimation of wind turbine blade forces with a state-augmented kalman filter. In: 48th AIAA aerospace sciences meeting. Orlando, FL; 2010. http://dx.doi.org/10.2514/6.2010-1580.

[37] Fischer A, Madsen HA. Investigation of the maximum load alleviation potential using trailing edge flaps controlled by inflow data. The Science of Making Torque from Wind. Oldenburg, Germany; 2012.

[38] Rachidi F, Rubinstein M, Montanya J, Bermúdez J-L, Rodriguez Sola R, Sola G, et al. A review of current issues in lightning protection of new-generation wind-turbine blades. IEEE Trans Ind Electron 2008;55:2489–96. http://dx.doi.org/10.1109/TIE.2007.896443.

[39] Berg J, Barone M, Resor B. Field test results from the Sandia SMART rotor. In: 51st AIAA aerospace sciences meeting. Grapevine, TX; 2013. http://dx.doi.org/10.2514/6.2013-1060.

[40] Bir G, Jonkman J. Aeroelastic instabilities of large offshore and onshore wind turbines. J Phys Conf Ser 2007;75:012069. http://dx.doi.org/10.1088/1742-6596/75/1/012069.

[41] Jonkman J, Butterfield S, Musial W, Scott G. Definition of a 5-MW reference wind turbine for offshore system development. Golden, CO: National Renewable Energy Laboratory. Report No.: NREL/TP-500-38060; 2009.

[42] Swartz RA, Lynch JP, Sweetman B, Rolfes R, Zerbst S. Structural monitoring of wind turbines using wireless sensor networks. Smart Struct Syst 2010;6:183–96.

[43] Anton SR, Taylor SG, Raby EY, Farinholt KM. Powering embedded electronics for wind turbine monitoring using multi-source energy harvesting techniques. Proc SPIE 2013;8690:869007–9. http://dx.doi.org/10.1117/12.2010637.

[44] Lim D-W, Mantell SC, Seiler PJ. Wireless structural health monitoring of wind turbine blades using an energy harvester as a sensor. In: Proceedings of the 32nd ASME wind energy symposium. MD: National Harbor; 2014. http://dx.doi.org/10.2514/6.2014-1395.

[45] Ling CS, Hewitt D, Burrow SG, Clare L, D.A.W. Barton, Wells DM, et al. Technological challenges of developing wireless health and usage monitoring systems. Proc SPIE 2013. http://dx.doi.org/10.1117/12.2008757 (86950K-1–86950K-12).

[46] Kanev S, van Engelen T. Wind turbine extreme gust control. Wind Energy 2010;13:18–35. http://dx.doi.org/10.1002/we.338.

[47] Johnson SJ, Larwood S, McNerney G, van Dam CP. Balancing fatigue damage and turbine performance through innovative pitch control algorithm. Wind Energy 2012;15:665–77. http://dx.doi.org/10.1002/we.495.

[48] Frederick M, Kerrigan EC, Graham JMR. Gust alleviation using rapidly deployed trailing-edge flaps. J Wind Eng Ind Aerodyn 2010;98:712–23. http://dx.doi.org/10.1016/j.jweia.2010.06.005.

[49] Rice JK, Verhaegen M. Robust and distributed control of a smart blade. Wind Energy 2010;13:103–16. http://dx.doi.org/10.1002/we.362.

[50] Bergami L, Poulsen NK. A smart rotor configuration with linear quadratic control of adaptive trailing edge flaps for active load alleviation. Wind Energy 2014. http://dx.doi.org/10.1002/we.1716.

[51] Lackner MA, van Kuik G. A comparison of smart rotor control approaches using trailing edge flaps and individual pitch control. Wind Energy 2010;13:117–34. http://dx.doi.org/10.1002/we.353.

[52] Berg JC, Resor BR, Paquette JA, White JR. SMART wind turbine rotor: design and field test. Albuquerque, NM: Sandia National Laboratories; 2014 (Report No.: SAND2014-0681).

[53] Verbruggen TW, Rademakers LWMM, Braam H. Fibre optic blade monitoring – development of a cost effective system for O&M optimization. Report No.: ECN-E-12-018. Energy Research Center of the Netherlands; 2012.

[54] Papadopoulos K, Morfiadakis E, Philippidis TP, Lekou DJ. Assessment of the strain gauge technique for measurement of wind turbine blade loads. Wind Energy 2000;3:35–65. http://dx.doi.org/10.1002/1099-1824(200001/03)3:1<35::AID-WE30>3.0.CO;2-D.

[55] Rumsey MA. An evaluation of sensing technologies in a wind turbine blade: some issues, challenges and lessons learned. Proc SPIE 2011;7979:79790G-15. http://dx.doi.org/10.1117/12.882024.

[56] Castaignet D, Barlas T, Buhl T, Poulsen NK, Wedel-Heinen JJ, Olesen NA, et al. Full-scale test of trailing edge flaps on a Vestas V27 wind turbine: active load reduction and system identification. Wind Energy 2014;17:549–64. http://dx.doi.org/10.1002/we.1589.

[57] Bossanyi EA, Fleming PA, Wright AD. Validation of individual pitch control by field tests on two- and three-bladed wind turbines. IEEE Trans Control Syst Technol 2013;21:1067–78. http://dx.doi.org/10.1109/TCST.2013.2258345.

[58] Giurgiutiu V. Piezoelectricity principles and materials. Encyclopedia of structural health monitoring. Chichester, West Sussex, UK: John Wiley & Sons, Ltd.; 2009.

[59] Bent AA, Hagood NW. Piezoelectric fiber composites with interdigitated electrodes. J Intell Mater Syst Struct 1997;8:903–19. http://dx.doi.org/10.1177/1045389×9700801101.

[60] Pierfort V. Finite element modeling of piezoelectric active structures [dissertation]. Brussels, Belgium: Université Libre de Bruxelles; 2001.

[61] Wilkie WK, Bryant RG, High JW, Fox RL, Hellbaum RF, Jalink A, et al. Low-cost piezocomposite actuator for structural control applications. Proc SPIE 2000;3991:323–34. http://dx.doi.org/10.1117/12.388175.

[62] Wickramasinghe V, Chen Y, Martinez M, Wong F, Kernaghan R. Design and verification of a smart wing for an extreme-agility micro-air-vehicle. Smart Mater Struct 2011;20:125007. http://dx.doi.org/10.1088/0964-1726/20/12/125007.

[63] Olson SP, Castracane J, Spoor RE. Piezoresistive strain gauges for use in wireless component monitoring systems. In: Proceedings of the IEEE sensors applications symposium. Atlanta, GA; 2008.

[64] Hulskamp AW, van Wingerden JW, Barlas T, Champliaud H, van Kuik GAM, Bersee HEN, et al. Design of a scaled wind turbine with a smart rotor for dynamic load control experiments. Wind Energy 2011;14:339–54. http://dx.doi.org/10.1002/we.424.

[65] van Wingerden J-W, Hulskamp A, Barlas T, Houtzager I, Bersee H, van Kuik G, et al. Two-degree-of-freedom active vibration control of a prototyped "Smart" rotor. IEEE Trans Control Syst Technol 2011;19:284–96. http://dx.doi.org/10.1109/TCST.2010.2051810.

[66] Barlas TK, van Wingerden W, Hulskamp AW, van Kuik GAM, Bersee HEN. Smart dynamic rotor control using active flaps on a small-scale wind turbine: aeroelastic modeling and comparison with wind tunnel measurements. Wind Energy 2013;16:1287–301. http://dx.doi.org/10.1002/we.1560.

[67] Udd E. Fiber optic smart structures. Proc IEEE 1996;84:884–94. http://dx.doi.org/10.1109/5.503144.

[68] Lopez-Higuera JM, Rodriguez Cobo L, Quintela Incera A, Cobo A. Fiber optic sensors in structural health monitoring. J Lightwave Technol 2011;29:587–608. http://dx.doi.org/10.1109/JLT.2011.2106479.

[69] Peters K. Polymer optical fiber sensors—a review. Smart Mater Struct 2011;20:013002. http://dx.doi.org/10.1088/0964-1726/20/1/013002.

[70] Schukar VG, Kadoke D, Kusche N, Münzenberger S, Gründer K-P, Habel WR. Validation and qualification of surface-applied fibre optic strain sensors

using application-independent optical techniques. Meas Sci Technol 2012;23:085601. http://dx.doi.org/10.1088/0957-0233/23/8/085601.
[71] Measures RM. Smart composite structures with embedded sensors. Compos Eng 1992;2:597–618. http://dx.doi.org/10.1016/0961-9526(92)90045-8.
[72] Cairns D, Palmer N, Ehresman J. Embedded sensors for composite wind turbine blades. In: Proceedings of the 51st AIAA/ASME/ASCE/AHS/ASC structures, structural dynamics, and materials conference. Orlando, FL; 2010. http://dx.doi.org/10.2514/6.2010-2822.
[73] Chen Y, Ni YQ, Ye XW, Yang HX, Zhu S. Structural health monitoring of wind turbine blade using fiber Bragg grating sensors and fiber optic rotary joint. Proc SPIE 2012;8345:834534–6. http://dx.doi.org/10.1117/12.914961.
[74] Lee JM, Hwang Y. A novel online rotor condition monitoring system using fiber Bragg grating (FBG) sensors and a rotary optical coupler. Meas Sci Technol 2008;19:065303. http://dx.doi.org/10.1088/0957-0233/19/6/065303.
[75] Peters K. Intensity-, interferometric-, and scattering-based optical-fiber sensors. Encyclopedia of structural health monitoring. Chichester, West Sussex, UK: John Wiley & Sons, Ltd.; 2009.
[76] Kuang KSC, Cantwell WJ. The use of plastic optical fibre sensors for monitoring the dynamic response of fibre composite beams. Meas Sci Technol 2003;14:736–45. http://dx.doi.org/10.1088/0957-0233/14/6/305.
[77] Sendrup P. Fundamentals for remote structural health monitoring of wind turbine blades – a preproject. Annex C – fibre transducer for damage detection in adhesive layers of wind turbine blades. Roskilde, Denmark: Risø National Lab. for Sustainable Energy. Report No.: Riso-R-1342; 2002.
[78] Kersey AD. A review of recent developments in fiber optic sensor technology. Opt Fiber Technol 1996;2:291–317. http://dx.doi.org/10.1006/ofte.1996.0036.
[79] Hill KO, Meltz G. Fiber Bragg grating technology fundamentals and overview. J Lightwave Technol 1997;15:1263–76. http://dx.doi.org/10.1109/50.618320.
[80] Liu HB, Liu HY, Peng GD, Chu PL. Strain and temperature sensor using a combination of polymer and silica fibre Bragg gratings. Opt Commun 2003;219:139–42. http://dx.doi.org/10.1016/S0030-4018(03)01313-0.
[81] Verbruggen TW. Load monitoring for wind turbines. Fibre optic sensing and data processing. Energy Research Center of the Netherlands. Report No.: ECN-E-09-071; 2010.
[82] Guemes JA, Menéndez JM. Response of Bragg grating fiber-optic sensors when embedded in composite laminates. Compos Sci Technol 2002;62:959–66. http://dx.doi.org/10.1016/S0266-3538(02)00010-6.
[83] Emmons MC, Karnani S, Trono S, Mohanchandra KP, Richards WL, Carman GP. Strain measurement validation of embedded fiber Bragg gratings. Int J Optomechatron 2010;4:22–33. http://dx.doi.org/10.1080/15599611003649984.
[84] Rademakers L, Verbruggen TW, van der Werff PA, Korterink H, Richon D, Rey P, et al. Fiber optic blade monitoring. In: Proceedings of the European wind energy conference. London; 2004.
[85] Kuhnt S, Wernicke J, Shadden J, Byars R. Advanced wind turbine controls input based on real time loads measured with fibre optical sensors embedded in rotor blades. In: Proceedings of the European wind energy conference. Athens, Greece; 2006.
[86] Schroeder K, Ecke W, Apitz J, Lembke E, Lenschow G. A fibre Bragg grating sensor system monitors operational load in a wind turbine rotor blade. Meas Sci Technol 2006;17:1167–72. http://dx.doi.org/10.1088/0957-0233/17/5/S39.
[87] Bang H, Jang M, Shin H. Structural health monitoring of wind turbines using fiber Bragg grating based sensing system. Proc SPIE 2011;7981:79812H–8H. http://dx.doi.org/10.1117/12.880654.
[88] Park S, Park T, Han K. Real-time monitoring of composite wind turbine blades using fiber Bragg grating sensors. Adv Compos Mater 2011;20:39–51. http://dx.doi.org/10.1163/092430410X504198.
[89] Derkevorkian A, Alvarenga J, Masri SF, Boussalis H, Richards WL. Computational studies of a strain-based deformation shape prediction algorithm for control and monitoring applications. Proc SPIE 2012;8343:83430F-10. http://dx.doi.org/10.1117/12.914579.
[90] Kim H-I, Han J-H, Bang H-J. Real-time deformed shape estimation of a wind turbine blade using distributed fiber Bragg grating sensors: strain-based shape estimation. Wind Energy 2013. http://dx.doi.org/10.1002/we.1644.
[91] Arsenault TJ, Achuthan A, Marzocca P, Grappasonni C, Coppotelli G. Development of a FBG based distributed strain sensor system for wind turbine structural health monitoring. Smart Mater Struct 2013;22:075027. http://dx.doi.org/10.1088/0964-1726/22/7/075027.
[92] Güemes A, Fernández-López A, Soller B. Optical fiber distributed sensing – physical principles and applications. Struct Health Monit 2010;9:233–45. http://dx.doi.org/10.1177/1475921710365263.
[94] Kreger ST, Gifford DK, Froggatt ME, Soller BJ, Wolfe MS. High resolution distributed strain or temperature measurements in single- and multi-mode fiber using swept-wavelength interferometry. Opt Fiber Sens, Cancun, Mexico 2006. http://dx.doi.org/10.1364/OFS.2006.ThE42.
[95] Kreger ST, Sang AK, Gifford DK, Froggatt ME. Distributed strain and temperature sensing in plastic optical fiber using Rayleigh scatter. Proc SPIE 2009;7316:73160A–8A. http://dx.doi.org/10.1117/12.821353.
[96] Pedrazzani JR, Klute SM, Gifford DK, Sang AK, Froggatt ME. Embedded and surface mounted fiber optic sensors detect manufacturing defects and accumulated damage as a wind turbine blade is cycled to failure. Baltimore, MD: SAMPE; 2012.
[97] Lally EM, Reaves M, Horrell E, Klute S, Froggatt ME. Fiber optic shape sensing for monitoring of flexible structures. Proc SPIE 2012;8345:83452Y–9Y. http://dx.doi.org/10.1117/12.917490.
[98] White JR, Adams DE, Rumsey MA, Paquette J. Estimation of wind turbine blade operational loading and deflection with inertial measurements. In: 47th AIAA aerospace sciences meeting. Orlando, FL; 2009. http://dx.doi.org/10.2514/6.2009-1407.
[99] White JR, Adams DE, Rumsey MA. Modal analysis of CX-100 rotor blade and Micon 65/13 wind turbine. In: Proceedings of the IMAC-XXVIII, vol. 1, Jacksonville, FL: Springer; 2010. p. 15–27. http://dx.doi.org/10.1007/978-1-4419-9716-6_2.
[100] Riziotis VA, Voutsinas SG. Aero-elastic modelling of the active flap concept for load control. In: Proceedings of the European wind energy conference. Brussels, Belgium; 2008.
[101] Rumsey MA, Paquette J, White JR, Werlink RJ, Beattie AG, Pitchford CW, et al. Experimental results of structural health monitoring of wind turbine blades. In: 46th AIAA aerospace sciences meeting. Reno, NV; 2008. http://dx.doi.org/10.2514/6.2008-1348.
[102] Kusnick J, Adams DE, Griffith DT. Wind turbine rotor imbalance detection using nacelle and blade measurements. Wind Energy 2014. http://dx.doi.org/10.1002/we.1696.
[103] Cherng A-P. Optimal sensor placement for modal parameter identification using signal subspace correlation techniques. Mech Syst Signal Process 2003;17:361–78. http://dx.doi.org/10.1006/mssp.2001.1400.
[104] Meyer J, Bischoff R, Feltrin G. Microelectromechanical systems (MEMS). Encyclopedia of structural health monitoring. Chichester, West Sussex, UK: John Wiley & Sons, Ltd.; 2009.
[105] Loh KJ, Lynch JP. Miniaturized sensors employing micro- and nanotechnologies. Encyclopedia of structural health monitoring. Chichester, West Sussex, UK: John Wiley & Sons, Ltd.; 2009.
[106] Martinez M, Rocha B, Li M, Shi G, Beltempo A, Rutledge R, et al. Load monitoring of aerospace structures utilizing micro-electro-mechanical systems for static and quasi-static loading conditions. Smart Mater Struct 2012;21:115001. http://dx.doi.org/10.1088/0964-1726/21/11/115001.
[107] Whale J, Fisichella C, Selig M. Correcting inflow measurements from HAWTs using a lifting-surface code. In: 37th aerospace sciences meeting. Reno, NV; 1999. http://dx.doi.org/10.2514/6.1999-40.
[108] Shipley DE, Miller MS, Robinson MC, Luttges MW, Simms DA Techniques for the determination of local dynamic pressure and angle of attack on a horizontal axis wind turbine. Golden, CO: National Renewable Energy Lab. Report No.: NREL/TP-442-7393; 1995.
[109] Kragh K, Hansen M. Individual pitch control based on local and upstream inflow measurements. In: 50th AIAA aerospace sciences meeting. Nashville, TN; 2012. http://dx.doi.org/10.2514/6.2012-1021.
[110] Kragh KA, Hansen MH, Henriksen LC. Sensor comparison study for load alleviating wind turbine pitch control. Wind Energy 2013. http://dx.doi.org/10.1002/we.1675.
[111] Barlas TK, van der Veen GJ, van Kuik GAM. Model predictive control for wind turbines with distributed active flaps: incorporating inflow signals and actuator constraints. Wind Energy 2012;15:757–71. http://dx.doi.org/10.1002/we.503.
[112] Bergami L, Gaunaa M. Stability investigation of an airfoil section with active flap control. Wind Energy 2010;13:151–66. http://dx.doi.org/10.1002/we.354.
[113] Heinz J, Sørensen NN, Zahle F. Investigation of the load reduction potential of two trailing edge flap controls using CFD. Wind Energy 2011;14:449–62. http://dx.doi.org/10.1002/we.435.
[114] Andersen PB. Advanced load alleviation for wind turbines using adaptive trailing edge flaps: sensoring and control [dissertation]. Risø National Laboratory for Sustainable Energy; 2010.
[115] Strike J, Hind M, Saini M, Naughton J, Wilson M, Whitmore S. Unsteady surface pressure reconstruction on an oscillating airfoil using the wiener deconvolution method. In: Proceedings of the 27th AIAA aerodynamic measurement technology and ground testing conference. Chicago, IL; 2010. http://dx.doi.org/10.2514/6.2010-4799.
[116] Olsen T, Lang E, Hansen AC, Cheney MC, Quandt G, VandenBosche J, et al. Low Wind Speed turbine project conceptual design study: advanced independent pitch control. Golden, CO: National Renewable Energy Laboratory. Report No.: NREL/SR-500-36755; 2004.
[117] Cooperman AM. Wind tunnel testing of microtabs and microjets for active load control of wind turbine blades [dissertation]. Davis, CA: University of California; 2012.
[118] Velte CM, Mikkelsen RF, Sørensen JN, Kaloyanov T, Gaunaa M. Closed loop control of a flap exposed to harmonic aerodynamic actuation. The science of making torque from wind. Journal of Physics, in press.
[119] Harris M, Hand M, Wright A. Lidar for turbine control. Golden, CO: National Renewable Energy Laboratory. Report No.: NREL/TP-500-39154; 2006.
[120] Harris M, Bryce DJ, Coffey AS, Smith DA, Birkemeyer J, Knopf U. Advance measurement of gusts by laser anemometry. J Wind Eng Ind Aerodyn 2007;95:1637–47. http://dx.doi.org/10.1016/j.jweia.2007.02.029.
[121] Schlipf D, Schuler S, Grau P, Allgöwer F, Kühn M. Look-ahead cyclic pitch control using lidar. The science of making torque from wind. 2010 < Available at: http://www.ist.uni-stuttgart.de/publications/bibs/ist/papers/ist:schlipf10a.pdf > .
[122] Dunne F, Pao L, Wright A, Jonkman B, Kelley N, Simley E. Adding feedforward blade pitch control for load mitigation in wind turbines: non-causal series expansion, preview control, and optimized FIR filter methods. In: 49th AIAA aerospace sciences meeting. Orlando, FL; 2011.

[123] Laks J, Pao L, Wright A, Kelley N, Jonkman B. The use of preview wind measurements for blade pitch control. Mechatronics 2011;21:668–81. http://dx.doi.org/10.1016/j.mechatronics.2011.02.003.
[124] Mirzaei M, Henriksen LC, Poulsen NK, Niemann HH, Hansen MH. Individual pitch control using LIDAR measurements. In: Proceedings of the 2012 IEEE international conference on control applications. Dubrovnik, Croatia; 2012. http://dx.doi.org/10.1109/CCA.2012.6402691.
[125] Schlipf D, Fleming P, Haizmann F, Scholbrock A, Hofsäß M, Wright A, et al. Field testing of feedforward collective pitch control on the CART2 using a nacelle-based lidar scanner. The science of making torque from wind. Journal of Physics, in press.
[126] Elorza I, Iribas M, Miranda E. On the feasibility and limits of extreme load reduction for wind turbines via advanced sensing: a LIDAR case study. In: Proceedings of the American Control Conference. Washington, DC; 2013.
[127] Schlipf D, Schlipf DJ, Kühn M. Nonlinear model predictive control of wind turbines using LIDAR. Wind Energy 2013;16:1107–29. http://dx.doi.org/10.1002/we.1533.
[128] Wang N, Johnson KE, Wright AD. Comparison of strategies for enhancing energy capture and reducing loads using LIDAR and feedforward control. IEEE Trans Control Syst Technol 2013;21:1129–42. http://dx.doi.org/10.1109/TCST.2013.2258670.
[129] Pace A, Johnson K, Wright A. Preventing wind turbine overspeed in highly turbulent wind events using disturbance accommodating control and light detection and ranging. Wind Energy 2014. http://dx.doi.org/10.1002/we.1705.
[130] Verwaal NW, van der Veen GJ, van Wingerden JW. Predictive control of an experimental wind turbine using preview wind speed measurements. Wind Energy 2014. http://dx.doi.org/10.1002/we.1702.
[131] Simley E, Pao LY, Frehlich R, Jonkman B, Kelley N. Analysis of light detection and ranging wind speed measurements for wind turbine control. Wind Energy 2014;17:413–33. http://dx.doi.org/10.1002/we.1584.
[132] Peña A, Hasager CB, Lange J, Anger I, Badger M, Bingöl F, et al. Remote sensing for wind energy. Roskilde, Denmark: DTU Wind Energy; 2013.
[133] Bossanyi E. Un-freezing the turbulence: application to LiDAR-assisted wind turbine control. IET Renew Power Gener 2013;7:321–9. http://dx.doi.org/10.1049/iet-rpg.2012.0260.
[134] Schlipf D, Trabucchi D, Bischoff O, Hofsäß M, Mann J, Mikkelsen T, et al. Testing of frozen turbulence hypothesis for wind turbine applications with a scanning LIDAR system. In: Proceedings of the international symposium on advancement of boundary layer remote sensing. Paris, France; 2010.
[135] Dunne F, Schlipf D, Pao LY. Comparison of two independent lidar-based pitch control designs. Golden, CO: National Renewable Energy Laboratory. Report No.: NREL/SR-5000-55544; 2012.
[136] Ozdemir AA, Seiler P, Balas GJ. Design tradeoffs of wind turbine preview control. IEEE Trans Control Syst Technol 2013;21:1143–54. http://dx.doi.org/10.1109/TCST.2013.2261069.
[137] Richards WL, Parker AR, Ko WL, Piazza A, Chan P. Application of fiber optic instrumentation. Chapter 6 – recent examples of large scale FOSS testing (RTO-AG-160 AC/323(SCI-228)TP/446. . NATO Science and Technology Organization; 2012.
[138] Lee B. Review of the present status of optical fiber sensors. Opt Fiber Technol 2003;9:57–79. http://dx.doi.org/10.1016/S1068-5200(02)00527-8.
[139] Barbarino S, Bilgen O, Ajaj RM, Friswell MI, Inman DJ. A review of morphing aircraft. J Intell Mater Syst Struct 2011;22:823–77. http://dx.doi.org/10.1177/1045389 × 11414084.
[140] Klute S, Duncan R, Fielder R, Butler G, Mabe J, Sang A, et al. Fiber-optic shape sensing and distributed strain measurements on a morphing chevron. In: 44th AIAA aerospace sciences meeting. Reno, NV; 2006. http://dx.doi.org/10.2514/6.2006-624.
[141] Backman D, Martinez M. Validation of a structural health and loads monitoring platform using digital image correlation. In: Proceedings of the 27th ICAF symposium. Jerusalem; 2013.
[142] Ozbek M, Rixen DJ, Erne O, Sanow G. Feasibility of monitoring large wind turbines using photogrammetry. Energy 2010;35:4802–11. http://dx.doi.org/10.1016/j.energy.2010.09.008.
[143] Paulsen US, Erne O, Schmidt T. Wind Turbine Operational and Emergency Stop Measurements Using Point Tracking Videogrammetry. In: Proceedings of the SEM annual conference. Albuquerque, NM; 2009.
[144] Winstroth J, Seume J. Wind turbine rotor blade monitoring using digital image correlation: assessment on a scaled model. In: Proceedings of the 32nd ASME wind energy symposium. MD: National Harbor; 2014. http://dx.doi.org/10.2514/6.2014-1396.
[145] Burner AW, Lokos WA, Barrows DA. Aeroelastic deformation: adaptation of wind tunnel measurement concepts to full-scale vehicle flight testing. Langley Research Center: NASA. Report No.: RTO-MP-AVT-124; 2005.
[146] Madsen HA, Jensen L, Bak C, Paulsen US, Gaunaa M, Fuglsang P, et al. The DAN-AERO MWexperiments. (Final report). Roskilde, Denmark: Risø National Lab for Sustainable Energy; 2010 (Report No.: Riso-R-1726).
[147] Medina P, Singh M, Johansen J, Rivera Jove A, Machefaux E, Fingersh LJ, et al. Aerodynamic and performance measurements on a SWT-2.3-101 wind turbine. Anaheim, CA: WINDPOWER; 2011.
[148] Medina P, Singh M, Johansen J, Jove A, Fingersh L, Schreck S. Inflow characterization and aerodynamics measurements on a SWT-2.3-101 wind turbine. In: 50th AIAA aerospace sciences meeting. Nashville, TN; 2012. http://dx.doi.org/10.2514/6.2012-230.
[149] Angelou N, Mikkelsen T, Hansen KH, Sjöholm M, Harris M. LIDAR wind speed measurements from a rotating spinner (SpinnerEx 2009). Kgs. Lyngby, Denmark: Technical University of Denmark. Report No.: Risø-R-1741; 2010.
[150] Mikkelsen T, Hansen KH, Angelou N, Sjöholm M, Harris M, Hadley P, et al. Lidar wind speed measurements from a rotating spinner. In: Proceedings of the European wind energy conference. Warsaw, Poland; 2010.
[151] Mikkelsen T, Angelou N, Hansen K, Sjöholm M, Harris M, Slinger C, et al. A spinner-integrated wind lidar for enhanced wind turbine control. Wind Energy 2013;16:625–43. http://dx.doi.org/10.1002/we.1564.
[152] Hand MM, Johnson KE, Fingersh LJ, Wright AD. Advanced control design and field testing for wind turbines at the National Renewable Energy Laboratory. Denver, CO: World Renewable Energy Congress VIII; 2004.
[153] Wright AD, Fingersh LJ, Stol KA. Designing and testing controls to mitigate tower dynamic loads in the controls advanced research turbine. In: Proceedings of the 45th AIAA aerospace sciences meeting. Reno, NV; 2007. http://dx.doi.org/10.2514/6.2007-1021.
[154] Bossanyi E, Savini B, Iribas M, Hau M, Fischer B, Schlipf D, et al. Advanced controller research for multi-MW wind turbines in the UPWIND project. Wind Energy 2012;15:119–45. http://dx.doi.org/10.1002/we.523.
[155] Johnson KE, Fingersh LJ, Wright AD. Controls advanced research turbine: lessons learned during advanced controls testing. Golden, CO: National Renewable Energy Laboratory. Report No.: TP-500-38130; 2005.
[156] Johnson KE, Fleming PA. Development, implementation, and testing of fault detection strategies on the National Wind Technology Center's controls advanced research turbines. Mechatronics 2011;21:728–36. http://dx.doi.org/10.1016/j.mechatronics.2010.11.010.
[157] Scholbrock A, Fleming P, Fingersh L, Wright A, Schlipf D, Haizmann F, et al. Field testing lidar-based feed-forward controls on the NREL controls advanced research turbine. In: 51st AIAA aerospace sciences meeting. Grapevine, TX; 2013. http://dx.doi.org/10.2514/6.2013-818.
[158] Castaignet D, Wedel-Heinen JJ, Kim T, Buhl T, Poulsen NK. Results from the first full scale wind turbine equipped with trailing edge flaps. In: Proceedings of the 28th AIAA applied aerodynamics conference. Chicago, IL; 2010. http://dx.doi.org/10.2514/6.2010-4407.
[159] Castaignet D, Couchman I, Poulsen NK, Buhl T, Wedel-Heinen JJ. Frequency-weighted model predictive control of trailing edge flaps on a wind turbine blade. IEEE Trans Control Syst Technol 2013;21:1105–16. http://dx.doi.org/10.1109/TCST.2013.2260750.
[160] Berg D, Berg J, Wilson D, White J, Resor B, Rumsey M. Design, fabrication, assembly and initial testing of a SMART rotor. In: 49th AIAA aerospace sciences meeting. Orlando, FL; 2011. http://dx.doi.org/10.2514/6.2011-636.
[161] Berg JC, Barone MF, Yoder NC. SMART wind turbine rotor: data analysis and conclusions. Sandia National Laboratories: Albuquerque, NM. Report No.: SAND2014-0712. ; 2014.
[162] Bernhammer LO, De Breuker R, van Kuik GAM, Berg J, van Wingerden J-W. Model validation and simulated fatigue load alleviation of SNL smart rotor experiment. In: 51st AIAA aerospace sciences meeting. Grapevine, TX; 2013. http://dx.doi.org/10.2514/6.2013-316.